Received: 18 April 2024 | Revised: 20 November 2024 | Accepted: 27 November 2024

DOI: 10.1111/ppl.70026

ORIGINAL RESEARCH

Physiologia Plantarum

A role for root carbonic anhydrase βCA4 in the bicarbonate tolerance of *Arabidopsis thaliana*

Laura Pérez-Martín[1†] | Maria-José Almira[1†] | Laura Estrela-Muriel[1] | Roser Tolrà[1] | Lourdes Rubio[2] | Charlotte Poschenrieder[1] | Silvia Busoms[1]

[1]Department of Animal Biology, Plant Biology and Ecology; Plant Physiology Lab, Universitat Autònoma de Barcelona, Barcelona, Spain

[2]Department of Botany and Plant Physiology, Universidad de Málaga, Málaga, Spain

Correspondence
Silvia Busoms,
Email: silvia.busoms@uab.cat

Funding information
Ministry of Science, Innovation and Universities (Ministerio de Ciencia de España), Grant/Award Number: PID2019-104000RB-I00

Edited by V. Arbona

Abstract

Carbonic anhydrases (CAs) are the main enzymes handling bicarbonate in the different cell compartments. This study analyses the expression of CAs in roots of *Arabidopsis thaliana* demes differing in tolerance to bicarbonate: the tolerant $A1_{(C+)}$ deme and the sensitive deme, $T6_{(C-)}$. Exposure to 10 mM NaCl caused a transient depolarization of the root cell membranes, and in contrast, the supply of 10 mM $NaHCO_3$ caused hyperpolarization. This hyperpolarization was much stronger in $A1_{(C+)}$ than in $T6_{(C-)}$. Acetazolamide (AZ), a specific inhibitor of CAs, abolished the hyperpolarizing effect in $A1_{(C+)}$, indicating the implication of CAs in this fast membrane response. The time-dependent (3 to 72 h) expression profiles of 14 CAs in roots of $A1_{(C+)}$ and $T6_{(C-)}$ exposed to either control (0 mM $NaHCO_3$, pH 5.9), or bicarbonate (10 mM $NaHCO_3$,pH 8.3) conditions revealed a bicarbonate specific upregulation of *BCA4.1* (from 3 to 12 h) in $A1_{(C+)}$. Contrastingly, in $T6_{(C-)}$ *BCA4.1* was downregulated by $NaHCO_3$. Exclusively in $A1_{(C+)}$, the enhanced expression of *BCA4.1* under bicarbonate was parallelled by an increase of *PIP1,3*, *SLAH1*, *SLAH3*, *AHA2*, and *FRO2* gene expression levels. Under HCO_3^- exposure, a *bca4* knockout mutant had a lower number of lateral roots, lower root diameters, and higher root lipid peroxidation than the WT. These results indicate that bicarbonate-induced root membrane hyperpolarization is the fast (minutes) initial signalling event in the tolerance response. This is followed by the specific upregulation of *BCA4.1* and genes involved in H_2O and CO_2 transport, apoplast acidification, and iron acquisition.

1 | INTRODUCTION

Alkaline soils currently cover more than 30% of the earth surface, especially in arid and semi-arid areas such as the Mediterranean (Wahba et al., 2019). Under the prevailing and future climate change scenarios an aggravation of crop land alkalinization is foreseen (Hassani et al., 2021) and breeding for alkaline tolerant crops is an urgent mission.

Limestone soils, alkaline and alkaline saline soils largely differ in their physical and chemical properties, and the diverse constraints they impose on crop performance increase as pH and sodicity build up. However, a common characteristic is the high concentration of bicarbonate in their soil solutions. The adverse effects of bicarbonate on sensitive crop plants have mainly been considered by its repercussions on iron deficiency and, to a lesser extent, on other mineral nutrient deficiencies like nitrogen (N), potassium (K), magnesium (Mg), Zinc (Zn), manganese (Mn), molybdenum (Mo), copper (Cu) and zinc (Zn) deficiency.

† Contributed equally

Chalk chlorosis is a typical symptom of bicarbonate-induced iron deficiency in calcifuge species cultivated on calcareous soils (Tagliavini and Rombolà, 2001). Several mechanisms are responsible for this Fe deficiency: low Fe availability in soils with alkaline pH, interference of carbonate/bicarbonate with the iron mobilization strategy 1 of dicot species, hampering the activity of FERRIC REDUCTASE OXIDASE 2 (FRO2), the iron reductase that requires acid pH for optimal function, or the inhibition of Fe transport from roots to shoots (Wang et al., 2020).

Apoplastic pH homeostasis is achieved by collaboration between the plasma membrane H^+-ATPase (AHA) and homogalacturonans, the negatively charged cell wall pectins that can bind protons (Xu and Yu, 2023). Thus, bicarbonate tolerance is intimately related to AHA activity. Carbonate/bicarbonate, by its buffer capacity, may efficiently counteract the Fe acquisition strategy based on rhizosphere acidification. The exudation of flavonoid–type phenolics able to chelate Fe even under alkaline pH conditions is a major adaptive mechanism for plant performance on carbonate-rich soil (Terés et al., 2019; Vélez-Bermúdez and Schmidt, 2023). Fe deficiency responses on the genetic and molecular level have attracted much research effort, and the basic mechanisms of Fe acquisition and transport are getting highly established (Riaz and Guerinot, 2021). However, the fate of bicarbonate in plants is more concealed (Poschenrieder et al., 2018).

Under exposure to HCO_3^-, a strong inhibition of nitrate uptake by roots has been observed (Al-Mansouri and Alhendawi, 2014). Such inhibition could be caused by competition between HCO_3^- and other anions for transport mechanisms with low anion specificity (Poschenrieder et al., 2018). Anion channels in plants have mainly been studied in guard cells and are less characterized in roots. However, in Arabidopsis and soy, SLAC/SLAHs are reported to be nitrate conductive in roots, and the overexpression of SLAH3 has been associated with bicarbonate tolerance (Qiu et al., 2016; Zhang et al., 2016; Duan et al., 2018). Moreover, both the nitrate deficiency and the changes in root hydraulic conductivity caused by bicarbonate stress can alter the regulation of plasma membrane intrinsic proteins (PIPs; Di Pietro et al., 2013). In fact, the phosphorylation of the aquaporin PIP2 is essential for H_2O_2 extracellular export under alkaline conditions (Zhang et al., 2023).

Carbonic anhydrases (CAs) are the main enzymes handling bicarbonate inside and outside plant cells (DiMario et al., 2017, 2018; Ignatova et al., 2019). The role of CAs in carbon concentration mechanisms in aquatic photosynthetic organisms is well established (Raven et al., 2011; Kupriyanova et al., 2023). Leaf CAs have recently gained much attention not only in C4 photosynthesis (Zhou et al., 2024) but also in terrestrial C3 plants due to their potential role in mesophyll conductance and photosynthesis, especially under stress conditions (Momayezzi et al., 2020; Weerasooriya et al., 2024). In carbonate-rich karst environments, drought-induced stomatal closure may strongly limit CO_2 diffusion into the leaves. In plants adapted to such extreme conditions, the overall photosynthesis rate is considerably decreased, but CA activity is strongly enhanced, and HCO_3^--derived CO_2 can contribute up to 30% of the photosynthetic C assimilation (Wu and Xing, 2012; Wu and Wu, 2022). Enhancing CA in response to HCO_3^- exposure has been highlighted as an important trait for adaptation to the karst environment (Müller et al., 2014).

Nonetheless, the information on the mechanisms behind the potential role of root CAs in the tolerance of terrestrial plants to high soil bicarbonate is poor. The elucidation is hampered by the large number of different CAs located in different cell compartments in plants, and the still fragmentary identification of the corresponding genes in bicarbonate tolerant species. Best characterized from the genetic point of view is the model plant *Arabidopsis thaliana*. The species contains 19 CA genes: eight α, six β, and five γ CAs (DiMario et al., 2018). AtγCAs are localized in the mitochondria and are mainly involved in photorespiration processes (Parisi et al., 2004). Thus, in this study, we focus on α and β CAs that are found in cell walls, the plasma membrane, the cytosol, and plastids and are highly expressed in roots (Fabre et al., 2007).

Arabidopsis thaliana is increasingly employed in evolutionary and ecological studies. Patterns of natural genetic variation and the forces that shape them have been studied mostly at global and regional scales (Stenøien et al., 2005; Schmid et al., 2006; Beck et al., 2008). Local populations have been shown to be strongly differentiated even when they are geographically close (Bergelson et al., 1998; Bakker et al., 2006). Genotypic and phenotypic diversity of natural subpopulations of *A. thaliana* from the Northeast of Spain (Catalunya) were large enough to provide a scenario for exploring tolerance mechanisms to soil carbonate (Terés et al., 2017; Busoms et al., 2023), proving the effects of environmental heterogeneity in creating diversity patterns even at local scale. The term "*A. thaliana* deme" was established for these subpopulations, referring to "a small group or stand of *A. thaliana* plants growing in relatively homogeneous ecological conditions and separated from other groups by at least 35 m" (Busoms et al., 2015). Two demes, $A1_{(C+)}$ and $T6_{(C-)}$, with differential tolerance to moderate soil carbonate concentrations, showed differential growth, reproduction, and photosynthetic efficiency due to differences in both nutrient profiles and degree of membrane damage under bicarbonate stress (Pérez-Martín et al., 2021).

With the aim of shedding light on the role of plasma membrane CAs in plant bicarbonate tolerance and taking advantage of these naturally evolved differences in tolerance to carbonated soils, the present study explores the influence of bicarbonate on the plasma membrane potential of root cells and the expression levels of α and βCAs in roots of these contrasting *A. thaliana* demes. Our working hypothesis was that the tolerant $A1_{(C+)}$ may better control bicarbonate toxicity by higher expression levels of carbonic anhydrases.

2 | MATERIALS AND METHODS

2.1 | Plant materials

Seeds of contrasting phenotype lines from $A1_{(C+)}$, an alkaline-moderate tolerant deme, and $T6_{(C-)}$, an alkaline sensitive deme, were collected from field cultivated plants and stored under cold (4°C) and

dry conditions until the beginning of the experiments. Seeds of the mutant knock-out line (ecotype Columbia) carrying T-DNA insertions in βCA4, *bca4.1* (WiscDsLox508D11), and the reference Col-0 were obtained from the Nottingham Arabidopsis Stock Centre (NASC).

2.2 | Growth conditions

Seeds were surface sterilized by soaking in 30% Clorox bleach and a drop of Tween-20 for 10 minutes and then rinsed six times in sterile 18 MΩ milli-Q water. For stratification, seeds were placed in Petri dishes containing filter paper soaked with 3 mL KNO_3 solution (10^{-3} M) at 4°C and dark conditions for one week.

For electrophysiological studies, after stratification seeds from each deme were sown in plates under a flow cabinet with sterile material. The plates contained ½ MS + phyto-agar 0.6%, at pH 5.9. They were placed into a growth chamber (12 h light/12 h dark, 150 μmol $cm^{-2}{\cdot}s^{-1}$, 40% humidity and 25°C) where the seedlings were grown for seven days.

For other experiments, *A. thaliana* plants were grown in hydroponics. After stratification, seeds were sown in 0.2 mL tubes containing 0.6% agar prepared in ½ Hoagland nutrient solution (HS; pH 5.9) and placed in the growth chamber under the conditions described above. After root emergence, the bottoms of the tubes containing seedlings were cut off and the tubes were placed in 150 mL hydroponic containers with aerated ½ Hoagland solution (pH 5.9). 15-days old plants were separated in two different treatments: control (C: ½ HS at pH 5.9) and bicarbonate (Bic: ½HS with 10 mM $NaHCO_3$ at pH 8,3) until their harvest. Solutions were buffered with different proportions of MES and BTP depending on the desired final pH. The nutrient solutions were changed every three days.

2.3 | Phenotypic analysis

After 10 days of treatment with 0 mM (pH 5.9) or 10 mM $NaHCO_3$ (pH 8,3), six $A1_{(C+)}$, $T6_{(C-)}$, Col-0 and *bca4* plants per treatment were harvested for phenotypic analysis. Mini-Pam II (Walz GmbH) was used for measuring photosynthetic efficiency in leaves, and leaf chlorophyll concentration was measured using a CCM-300 chlorophyll content meter (Opti-Science). Morphology was assessed by scanning rosettes and roots with an Epson Expression 10000XL scanner and analyzed using the software WinRhizo Pro 2009c. Leaf area, number of leaves, number of lateral roots, number of forks and tips and average root diameter were analyzed.

For the thiobarbituric acid reactive substances (TBARs) analysis, 200 μL of 0.5% thiobarbituric acid (TBA) in 20% trichloroacetic acid (TCA) was added to 200 μL of the extract. The mixtures were heated at 95°C for 25 min and then quickly cooled in an ice bath. After centrifugation at 10 000 g for 6 min, the absorbance was recorded at 532 and 600 nm. Lipid peroxidation is expressed as nmol TBARs x g^{-1} FW.

2.4 | Root cell membrane potential measurements

Membrane potential was measured using the standard glass microelectrode technique (Felle, 1981). The microelectrodes were produced using 1.5 mm OD glass capillaries pulled in a David Kopf vertical puller (model 720, David Kpoft Instruments). The reference electrode was filled with 0.5 M KCl + agar 0.03% while the measurement electrode was filled with 0.5 M KCl. Both electrodes were connected to a high-impedance differential amplifier (FD223a). The measurement chamber was open on both sides allowing the approach of measure and reference electrodes to the root. A gravity-based flow-through system permitted controlled changes of the medium at a rate of 10 mL min^{-1}. This system kept the temperature, ionic concentration, and gases constant during the experiments. Microscope light (150 μmol photons m^{-2} s^{-1}) was on during the experiments. The signals from differences in root membrane potential were monitored on a chart recorder (Linseis L250E). Membrane potential measurements were made under continuous perfusion in epidermal root cells of 7-day old plate-cultivated seedlings. Seedlings were fixed to the measurement chamber and continuously perfused with a simplified bath solution (0.1 mM $CaCl_2$; 0.1 mM KCl, 10 mM Mes-BTP, pH 8.3) for at least 20 min before epidermal root cell impalement. After reaching a stable membrane potential value, NaCl or $NaHCO_3$ increasing concentrations, ranging from 0 to 10 mM, were added to the bath solution till membrane potential reached a new value, 3–5 min after each NaCl or $NaHCO_3$ addition. The influence of the inhibition of external carbonic anhydrases was studied monitoring the membrane potential response to the addition of 10 mM NaCl or $NaHCO_3$ in the presence of 0.1 mM acetazolamide (AZ). An AZ stock solution (10 mM) was prepared in 0.05 M NaOH. The addition of an equivalent volume of NaOH without the inhibitor had no effect on the measurements (Rubio et al., 2017).

2.5 | Relative gene expression

Hydroponically grown 15-days old $A1_{(C+)}$, $T6_{(C-)}$ seedlings were treated with 0 (pH 5.9) or 10 mM $NaHCO_3$ (pH 8,3) and harvested after 0, 3, 6, 24, 48, and 72 hours of exposure. Three plant roots were pooled to perform a replicate, and three replicates were taken from each deme and treatment. Root material was rinsed with deionized water and immediately frozen at −80°C.

RNA was extracted using a Maxwell plant RNA kit (Promega Corporation). After quality and quantity control, RNA was transcribed to cDNA using the iScriptTM cDNA Synthesis Kit (Bio-Rad). The cDNA was used as a template for quantitative PCRs using iTaq Universal SYBR Green Supermix (Bio-Rad). Real-time detection of fluorescence emission was performed on a CFX384 Real-Time System (Bio-Rad, Hercules, USA) using the following conditions: denaturalization step 10″ at 95°C followed by annealing and extension 30″ at 60°C. A total of 40 cycles were run. A melting curve was performed, increasing from 65.0°C to 95.0°C by 0.5°C each 5 seconds. Primers for *FRO2*, *IRT1*, *AHA2*, *αCAs* (1–8) and *βCAs* (1–6) were designed using the NCBI primer blast tool and they were purchased from Biolegio BV (Nijmegen, The Netherlands). The *Actin2* gene (AT3G18780) was used

as a housekeeping gene. The sequence of the primers is shown in Dataset S1. Plates were edited using the CFX manager version 3.1 software. The expression of the target gene relative to the expression of the reference gene was calculated using the $2^{-\Delta\Delta Ct}$ method (Livak and Schmittgen, 2001).

2.6 | Statistical analysis

Statistics and data visualization were performed using JMP Pro 13.2.1 (SAS Institute Inc.). In physiological measurements, the normal distribution of data was confirmed by Levene's test. Differences among treatments, demes, or time were analyzed by one-way ANOVA or the Least Square method. Post-hoc analyses were realized using the Tukey or Student t-test. The number of plants used in each experiment and the statistical analyses are provided in Dataset S2.

3 | RESULTS AND DISCUSSION

3.1 | *A. thaliana* deme responses to bicarbonate stress

Both *A. thaliana* demes clearly differed in their responses to bicarbonate stress. PSII efficiency measured as Fv/Fm ratio decreased considerably more by bicarbonate (10 mM $NaHCO_3$, pH 8,3) exposure in deme $T6_{(C-)}$ than in $A1_{(C+)}$ or in the reference accession Col-0 (Figure 1A). Root and leaf TBARs concentrations revealed higher bicarbonate–induced lipid peroxidation in $T6_{(C-)}$ than in $A1_{(C+)}$ or Col-0 (Figure 1B). These results confirm the previously reported bicarbonate sensitivity in $T6_{(C-)}$ and the contrasting tolerance in $A1_{(C+)}$ but do not reflect the intermediate sensitivity/tolerance, observed in Col-0 in terms of growth and fitness (Terés et al., 2019; Pérez-Martín et al., 2021). The elemental composition of the first 5 to 10 cm of soil notably fluctuates depending on the rainfall regime. *A. thaliana* seeds germinate after raining periods, but with the high evapotranspiration rates of the Mediterranean area, the surface soil where *A. thaliana* is rooting dries rapidly and the pH, bicarbonate, and Na^+ concentrations rise. We hypothesize that adapted plants like $A1_{(C+)}$ can perceive these changing conditions and respond quickly activating tolerance mechanisms, thus showing no symptoms of stress after several hours of exposure.

3.2 | Root cells plasma membrane potential

To further characterize the ion specificity of the observed differences, we compared the influence of NaCl and $NaHCO_3$ on the root cell plasma membrane potential of both demes at isomolar concentrations and under the same alkaline pH (8.3) conditions (Figure 2A, B). As expected, NaCl caused membrane depolarizations, that were higher in the case of $T6_{(C-)}$ at higher concentration. The NaCl-induced depolarizations in $A1_{(C+)}$ adjusted to a saturation curve showing a semi-saturation constant (3.1 ± 0.7 mM NaCl) in the range of assayed NaCl concentrations, while this was not the case in $T6_{(C-)}$ (Figure 2A). Contrastingly, equimolar $NaHCO_3$ exposure quickly caused a strong, transient hyperpolarization in $A1_{(C+)}$, while less hyperpolarization was observed in $T6_{(C-)}$ (Figure 2B). The different responses caused by NaCl and $NaHCO_3$ clearly demonstrate an anion-specific effect. It is well established that under NaCl stress, Na^+ uptake into root cells causes a quick transient depolarization of the membrane. This leads to the loss of cytosolic K^+ homeostasis in salt-sensitive plants, due to the activation of K^+ efflux channels like GORK for membrane repolarization. Instead, salt-tolerant plants are able to maintain K^+ homeostasis (Wu et al., 2018).

Contrastingly, when Na^+ was given in the form of $NaHCO_3$, membrane hyperpolarization occurred (Figure 2B). $NaHCO_3^-$ -induced

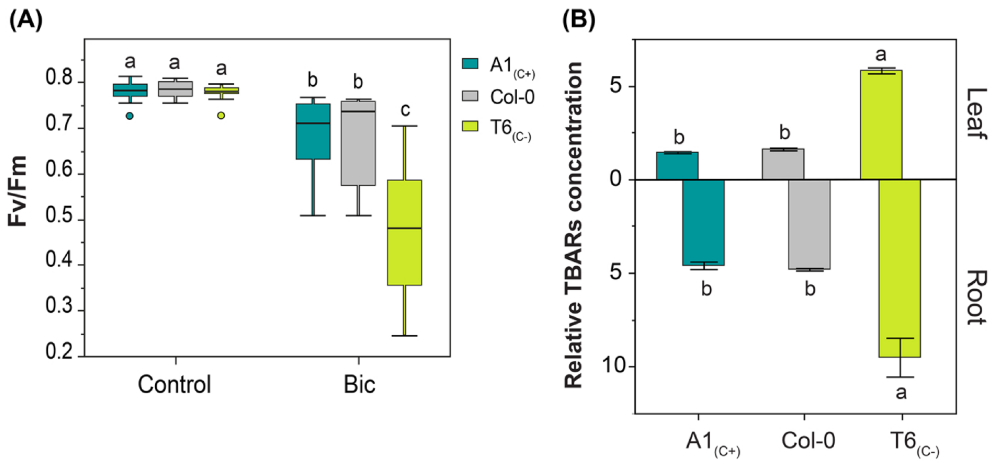

FIGURE 1 Photosynthesis efficiency and lipid peroxidation in Col-0, $A1_{(C+)}$ and $T6_{(C-)}$ under bicarbonate treatment. (A) Fv/Fm ratio (mean ± SE) of the reference accession Col-0, the tolerant $A1_{(C+)}$ and the sensitive $T6_{(C-)}$ demes under control (C: ½ HS at pH 5.9) and bicarbonate conditions (Bic: ½ HS with 10 mM $NaHCO_3$ at pH 8,3; $n = 6$). (B) Leaf (above) and root (below) relative TBARs concentration [(TBARs $_{Bic}$ / mean TBARs $_{C}$); mean ± SE] of Col-0, $A1_{(C+)}$ and $T6_{(C-)}$ ($n = 3$). Mean values with different letters indicate significant differences (ANOVA, Tukey's test, p-value <0.05).

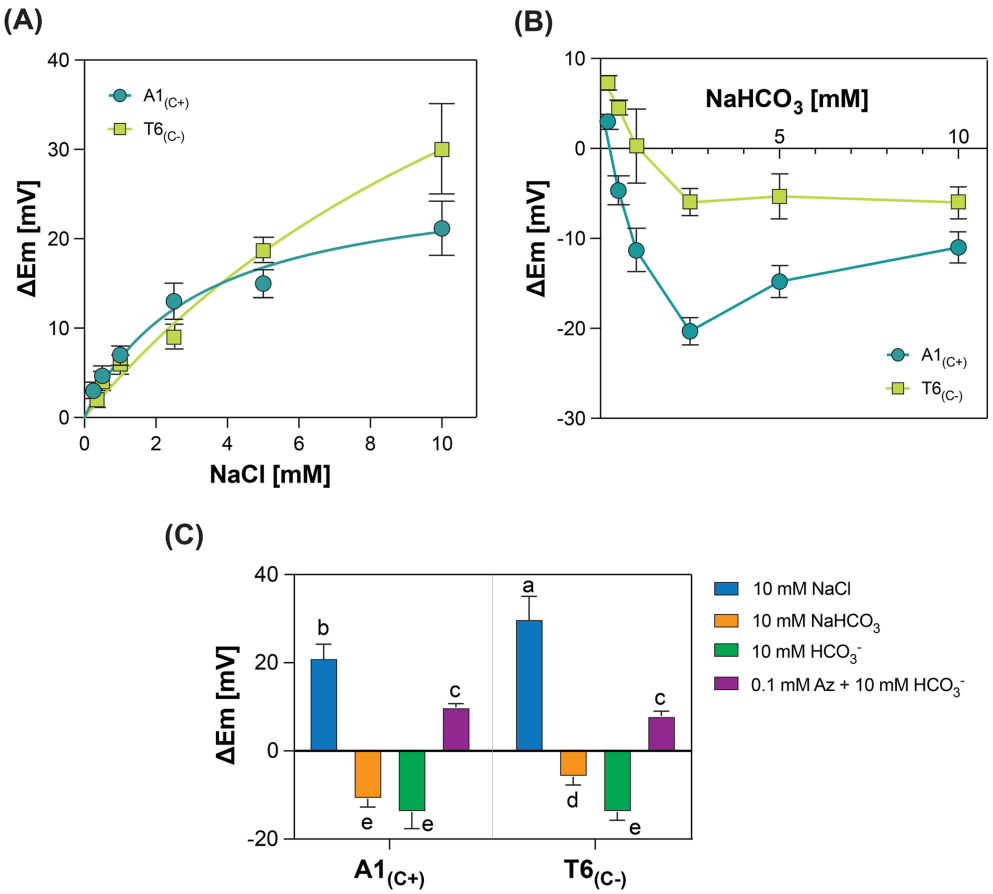

FIGURE 2 Effect of NaCl or $NaHCO_3$ additions on plasma membrane potential of epidermal root cells of $A1_{(C+)}$ and $T6_{(C-)}$. (A) Plasma membrane depolarizations induced by increasing NaCl concentrations. Values showed saturation kinetics and were fitted to a Michaelis–Menten model. (B) Plasma membrane hyperpolarizations induced by increasing $NaHCO_3$ concentrations. (C) Comparison of plasma membrane variations in response to the addition of 10 mM NaCl (blue bars), 10 mM $NaHCO_3$ (orange bars), and 10 mM HCO_3^- in the absence (green bars) or in the presence (purple bars) of 0.1 mM acetazolamide (AZ). Data are mean ± SE of at least five independent measurements. Different letters indicate significant differences (One way ANOVA, Tukey's test, p-value <0.001).

hyperpolarization was higher in $A1_{(C+)}$ than in $T6_{(C-)}$ at external concentrations from 1 to 10 mM. Hyperpolarization can be caused either by cation efflux or anion influx. To test whether bicarbonate uptake may be responsible for the strong hyperpolarization in A1, the influence of acetazolamide (AZ), a plasma membrane-impermeable inhibitor of CAs (Shitov et al., 2011) on the bicarbonate-induced membrane hyperpolarization was tested. The influence of Na^+ and HCO_3^- on membrane polarization is contrasting. Therefore, the exposition to $NaHCO_3$ would simultaneously promote both a Na^+-induced membrane depolarization and a membrane hyperpolarization if HCO_3^- is incorporated. To analyse these effects, during the treatment we changed the supply of 10 mM NaCl by 10 mM $NaHCO_3$ either in the absence or in the presence of 0.1 mM AZ. The presence of AZ completely abolished the hyperpolarizing effect of HCO_3^- (Figure 2C). Carbonic anhydrases catalyse the reversible hydration of CO_2 to HCO_3^- and H^+. Under the alkaline pH conditions of our experimental solution (pH 8.3), the supplied $NaHCO_3$ was mainly in the form of HCO_3^- and the CO_2 concentration was negligible. In the more acidic pH values of the apoplast and the cytosol, the proportion of CO_2 should be considerably higher. At present, no specific bicarbonate transporters have been identified in late divergent terrestrial plants, but HCO_3^- may enter cells by anion transporters (Poschenrieder et al., 2018). Membrane hyperpolarization could be caused by bicarbonate directly entering the cells. However, the cancellation of this hyperpolarization by AZ indicates that it was the consequence of CO_2 transformation into bicarbonate by intracellular carbonic anhydrase activity. Another possibility is that the activity of carbonic anhydrases activates proton extrusions, leading to membrane hyperpolarization. The consequent acidification of the apoplast would favor HCO_3^- dehydration and diffusion of CO_2 into the cell, where internal CAs may convert it to HCO_3^-, contributing to further membrane hyperpolarization. Future experiments analyzing cytosolic and external pH changes associated with this membrane hyperpolarization are required to clarify the underlying processes.

Regardless of the mechanism, an interesting result is that the CA-induced membrane hyperpolarization was much stronger in $A1_{(C+)}$ than in $T6_{(C-)}$ (Figure 2B). Such a fast differential response in the tolerant $A1_{(C+)}$ suggests that this membrane hyperpolarization could be the trigger of a signal transduction pathway leading to the quick activation of tolerance mechanisms in the $A1_{(C+)}$ deme. In fact, strong root cell hyperpolarization can activate Ca^{2+} influx channels in *A. thaliana* (Kiegle et al., 2000; Demichick et al., 2002), thus initiating stress signaling and activation of tolerance-related genes.

3.3 | Relative expressions of root α and β CAs and Fe-deficiency related genes

To explore this possibility, and following our initial hypothesis of a role for CAs in bicarbonate tolerance, we analyzed the time-dependent

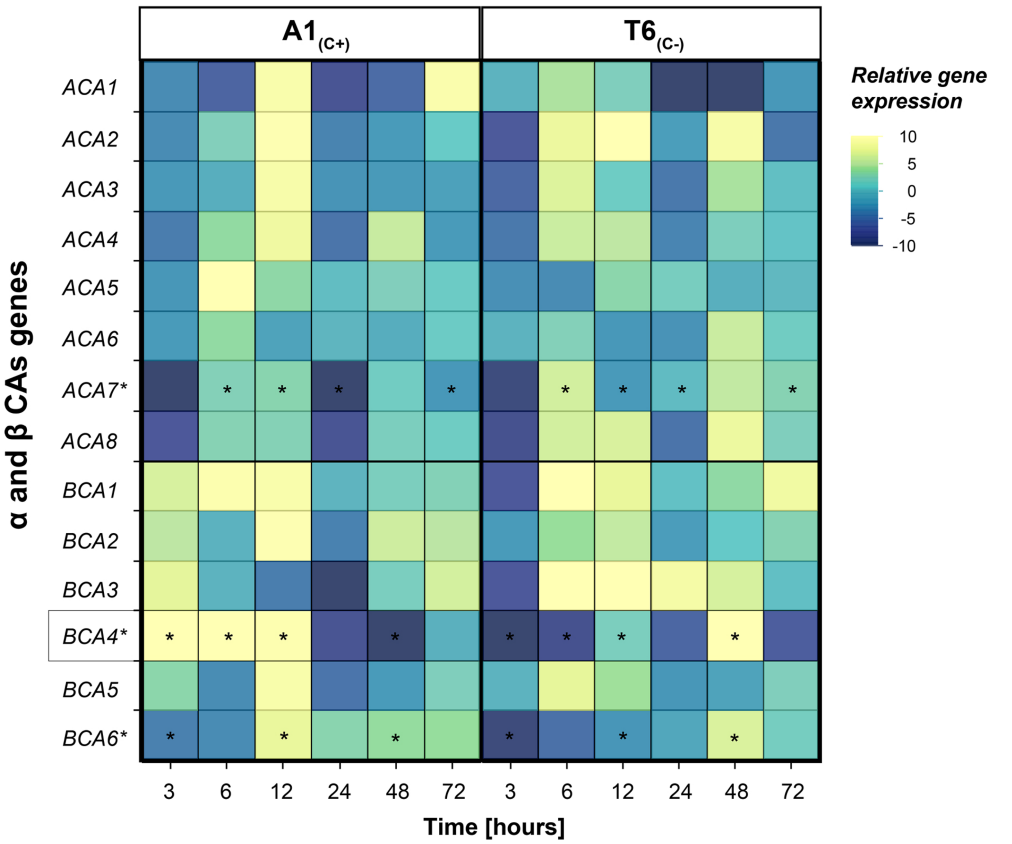

FIGURE 3 Root expression profiles of α and β CAs. Gene-expression heatmap of α and β CAs relative expression [log2 $(FC)_{Bic}$ / log2$(FC)_C$] in roots of $A1_{(C+)}$ and $T6_{(C-)}$ after 3, 6, 12, 24, 48 or 72 h of bicarbonate exposure. The colour scale indicates the expression levels (light yellow, high relative expression; dark blue, low relative expression). Asterisks indicate significant differences among demes (Least Square method, p-value <0.05).

root expressions of genes coding for α and β CAs, the main ones responsible for bicarbonate handling in the apoplast, plasma membrane and cytosol (DiMario et al., 2017; Figure 3). The most conspicuous differences between $A1_{(C+)}$ and $T6_{(C-)}$were the strong upregulation of *BCA4* during the first hours in the tolerant $A1_{(C+)}$, while the expression was downregulated in the sensitive $T6_{(C-)}$ (Figure 3). In *A. thaliana* βCA4 is encoded by At1G70410 (*BCA4*) which presents three splice variants. The primer used in our experiment amplifies At1G70410.2 coding for *BCA4.1* which is localized in the plasma membrane (DiMario et al., 2016). The role of plasma membrane-bound CAs in roots has not been identified so far. In stomata, the plasma membrane associated with βCA4 mediates the control of stomatal movement by CO_2 (Hu et al., 2015). βCA4–induced an increase of HCO_3^- concentration in the guard cells activating the S-type anion channel SLAC1 and therefore promoting anion efflux and stomatal closure (Tian et al., 2015).

Relative expression profiles of *AHA2*, *FRO2*, and *IRT1*, as the key players in root iron acquisition (Martín-Barranco et al., 2020), are shown in Figure 4. In $A1_{(C+)}$ the expressions of both *AHA2* (Figure 4A) and *FRO2* (Figure 4B) were upregulated by bicarbonate between 3 to 24 and 3 to 48 hours, respectively and declined thereafter. In $T6_{(C-)}$ *AHA2* expression remained unchanged upon bicarbonate exposure and *FRO2* expression was initially decreased and increased only slightly after 12 to 48 h exposure. *IRT1* expression peaked earlier in $T6_{(C-)}$ (6 to 12 h) than in $A1_{(C+)}$ (24 to 48 h) (Figure 4C). AHA2 is the key player in apoplastic and rhizosphere acidification required for Fe mobilization and the

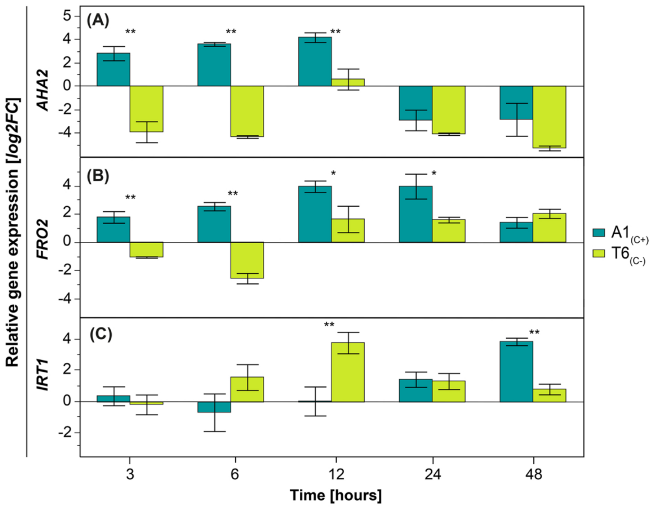

FIGURE 4 Root expression profiles of genes involved in iron acquisition in $A1_{(C+)}$ and $T6_{(C-)}$ under bicarbonate treatment. Relative expression [log2$(FC)_{Bic}$ / log2$(FC)_C$] of (A) *AHA2*, (B) *FRO2*, and (C) *IRT1* (mean ± SE) in roots of $A1_{(C+)}$ and $T6_{(C-)}$ after 3 or 48 h of bicarbonate exposure (n = 6). Asterisks indicate significant differences among demes (Least Square method, p-value <0.05).

activity of FRO2, the ferric chelate reductase. The quick upregulation of *AHA2* and *FRO2* prior to *IRT1* upregulation clearly support the superior ability of $A1_{(C+)}$ to mobilize and reduce Fe under alkaline conditions.

3.4 | Relative expression of the root S-type anion channel and aquaporin genes

In the view of the differential expression of *BCA4.1* in $A1_{(C+)}$ and $T6_{(C-)}$ and the role of this CA in the activation of *SLAC1* and stomatal closure (Wang et al., 2014), we compared the root expression profiles of *SLAH1* (SLAC1 homologue 1) and *SLAH3* (SALC1 homologue 3) in both demes under bicarbonate exposure (Figure 5). After 3 h exposure to bicarbonate both *SLAH1* and *SLAH3* were upregulated in $A1_{(C+)}$ but not in $T6_{(C-)}$. After 48 h *SLAH1* was downregulated in $A1_{(C+)}$ coincident with the downregulation of *BCA4.1* in this deme (Figure 3, 5). In Arabidopsis, SLAC1 is the founder member of a family of anion channels that comprises the homologs SLAC1 and SLAH3. They mediate chloride and nitrate transport in guard cells, and SLAH1, SLAH2 and SLAH3, are involved in root nitrate and chloride acquisition and in anion translocation to the aerial parts (Hedrich and Geiger, 2017). So far, the S-type anion channel SLAH3 in roots of *A. thaliana* has been related to acidity sensing, regulation of nitrogen-potassium homeostasis and Cl^- transport (Lehmann et al., 2021; Liu et al., 2023). Bicarbonate-induced expression of *GsSLAH3* has been observed in *Glycine soja* and overexpression of this gene in *A. thaliana* enhanced bicarbonate tolerance and the overexpressing lines accumulated higher nitrate concentrations (Duan et al., 2018). Our results give indirect support to the view that *BCA4.1* may be involved in the bicarbonate tolerance of *A. thaliana* deme $A1_{(C+)}$ by activating the transcription of S-type anion channels.

Moreover, in $A1_{(C+)}$ bicarbonate caused a strong upregulation of *PIP1,3* and *PIP2,5* after 3- and 48-hours exposure, respectively (Figure 5). No activation of aquaporins was observed in $T6_{(C-)}$. Besides water, aquaporins of the *PIP1* type can transport CO_2. Recently also *AtPIP2,5* has been shown to enhance the CO_2 entrance into yeast cells when co-expressed with carbonic anhydrase *AtCA1* more than 100-fold (Israel et al., 2022). Our results support the view that a cooperation between carbonic anhydrases, aquaporins, and S-type anion channels may not only have a function in stomatal closure, but also in roots providing tolerance to high substrate bicarbonate.

3.5 | *Bca4* mutant phenotyping

To get better insights into the possible role of *BCA4* in bicarbonate tolerance, the performance of the *BCA4.1* knockout mutant *(bca4)* exposed to bicarbonate (10 mM $NaHCO_3$ at pH 8,3 for 10 days) was analysed in comparison to the WT (Col-0), $A1_{(C+)}$ and $T6_{(C-)}$. Although bicarbonate exposure caused a reduction in the leaf area and leaf Fe concentration in all lines when compared to control conditions, the tolerant $A1_{(C+)}$ displayed higher growth and Fe translocation under bicarbonate than the rest. Moreover, the leaf number was significantly reduced under bicarbonate stress only in *bca4* and the sensitive $T6_{(C-)}$, but not in $A1_{(C+)}$ and Col-0 when compared to control (Figure 6A). Concerning root traits (Figure 6B), the effects of bicarbonate on the average root diameter were lower in the WT than in *bca4*, although both $A1_{(C+)}$ and $T6_{(C-)}$ resembled the mutant phenotype. Only the tolerant $A1_{(C+)}$ exhibited less alteration in lateral root formation under bicarbonate exposure. In addition, the mutant *bca4* developed higher root TBARs content than the rest of lines under bicarbonate conditions, followed by the sensitive $T6_{(C-)}$ (Figure 6B). The relatively small differences between the single loss-of-function mutant and WT phenotypes under bicarbonate exposure is probably due to the redundancy of the multiple CAs in *A. thaliana* (Bricks et al., 2006). Nonetheless, the influence of bicarbonate on root morphology and TBARs production in *bca4* supports a specific role for *BCA4.1* in iron acquisition. Enhanced root branching induced by Fe-deficiency may contribute to enhanced rhizosphere acidification and FRO2 activity, favouring iron reduction (Jin et al., 2008). In fact, in the carbonate tolerant $A1_{(C+)}$, the bicarbonate-induced activation of *BCA4.1* transcription (Figure 3) was accompanied by a higher enhancement of both *AHA2* and *FRO2* expression (Figure 4A, B) than in the carbonate sensitive $T6_{(C-)}$ where *BCA4.1* transcription was downregulated.

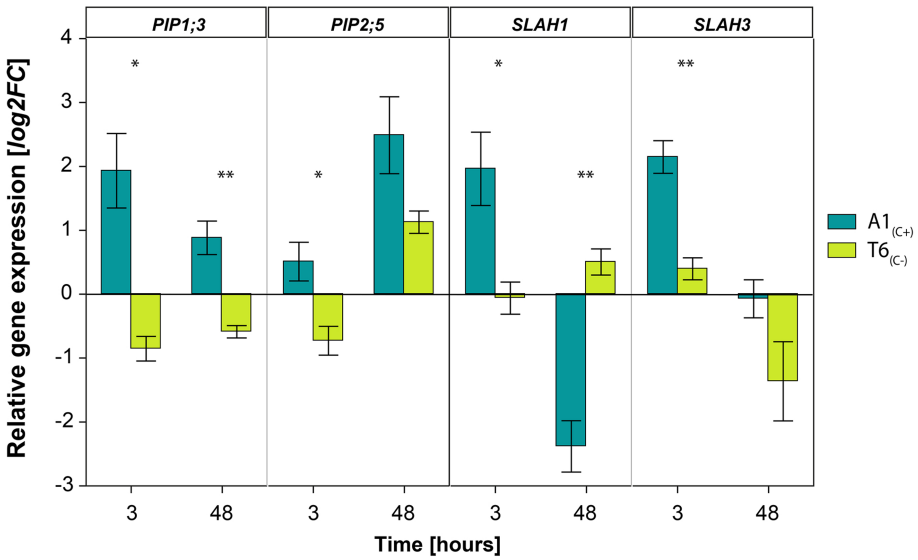

FIGURE 5 Root expression profiles of S-type anion channels and aquaporin genes in $A1_{(C+)}$ and $T6_{(C-)}$ under bicarbonate treatment. Relative expression $[\log2(FC)_{Bic} / \log2(FC)_C]$ of *PIP1;3*, *PIP2;5*, *SLAH1*, and *SLAH3* in roots of $A1_{(C+)}$ and $T6_{(C-)}$ after 3 or 48 h of bicarbonate exposure. Asterisks indicate significant differences among demes (ANOVA, Student *t*-Test, *: p-value <0.05; **: p-value <0.01).

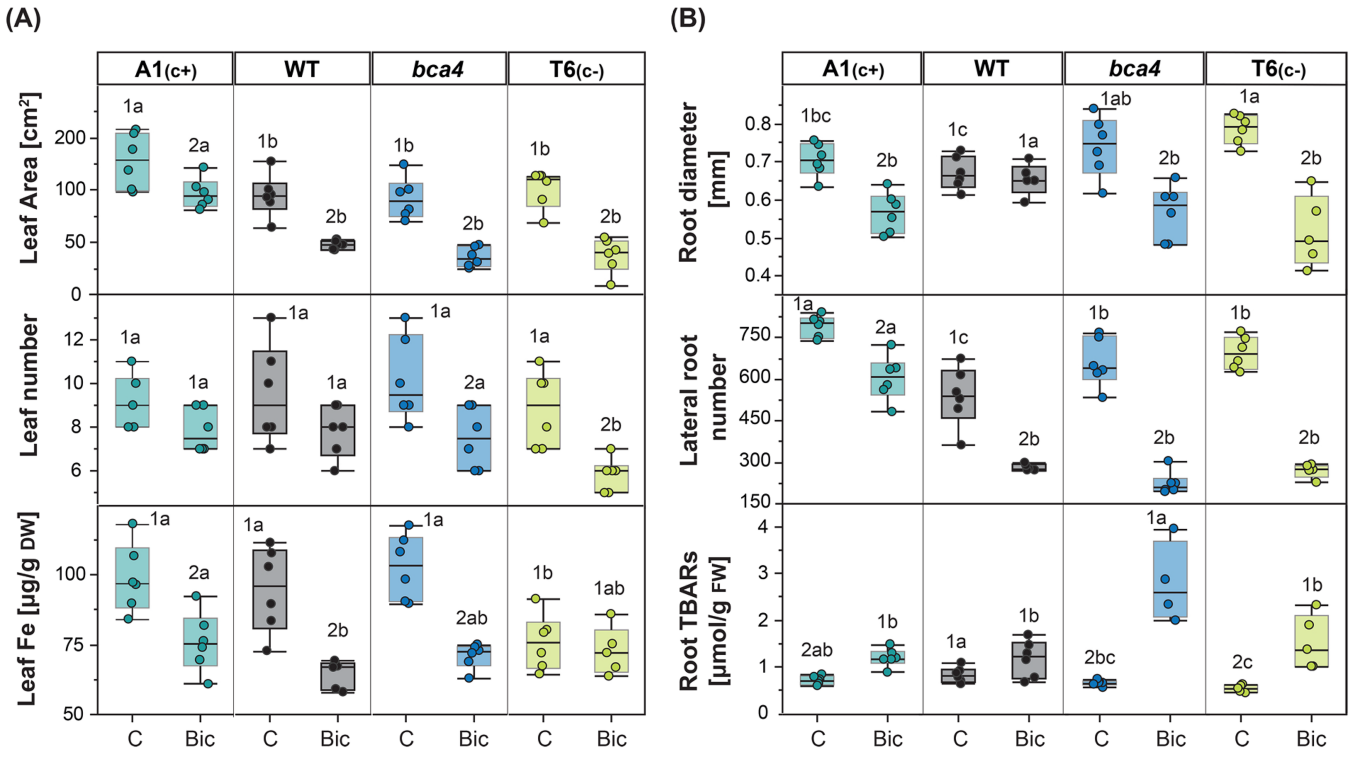

FIGURE 6 *BCA4.1* mutant phenotyping. Mean ± SE of (A) leaf area (cm^2), leaf number, and leaf Fe concentration (µg g^{-1} DW) and (B) root diameter (mm), lateral root number, and root TBARs content (µmol g^{-1} FW) of the *bca4* knockout mutant (blue), the WT Col-0 (black), $A1_{(C+)}$ (dark green), and $T6_{(C-)}$ (lemon green) under control (C: ½ HS at pH 5.9) and bicarbonate (Bic: ½ HS with 10 mM $NaHCO_3$ at pH 8,3) conditions (n = 6). Different numbers indicate significant differences among treatments and different letters indicate significant differences among accessions (ANOVA, Student *t*-Test, *p-value* <0.05).

4 | CONCLUSIONS

The strong, bicarbonate-induced hyperpolarisation of the root cell plasma membrane may act as a quick differential stress signalling mechanism in *A. thaliana* deme $A1_{(C+)}$ with naturally evolved tolerance to bicarbonate. This finding adds a new, still poorly explored piece to the model of Strategy 1 of Fe acquisition in plants exposed to alkaline soils. The coincidence of higher expressions in $A1_{(C+)}$ of *BCA4.1* with that of *AHA2* and *FRO2* along with the root phenotype of the *bca4* mutant provides circumstantial evidence for a role of *BCA4.1* in the activation of these mechanisms involved in Fe acquisition under bicarbonate stress.

The action of βCA4 in stomatal closure is well established. In guard cells, the high internal HCO_3^- concentrations activate aquaporins and anion channels. In analogy to this mode of action, the observation here of a bicarbonate-induced early upregulation of *BCA4.1*, *SLAH3*, *SLAH1*, and *PIP1,3* in the roots of $A1_{(C+)}$ suggests a cooperation of aquaporins and S-type anion channels mediated byβCA4 also in roots. Such a specific cooperation may be relevant in the bicarbonate tolerance strategies of plants. Further electrophysiological and molecular studies are required to see whether, and if so, how the initial membrane hyperpolarization is related to the subsequent upregulation of *BCA4.1*, *SLAH1*, *SLAH3*, *PIP1,2*, *AHA2*, and *FRO2*. Moreover, complementation studies should be conducted to assure that the sensitive phenotype observed in $T6_{(C-)}$ is mainly due to the lower expression of *BCA4.1*.

AUTHOR CONTRIBUTIONS

C.P., R.T. and S.B. conceived the study. L.P.M., M.A.C., and L.E.M. performed cultivations, lab experiments and analysis. L.P.M. and L.R. conducted electrophysiology experiments and data analysis. L.P.M., M.A.C., and S.B. performed the statistical and data analysis. C.P. and S.B. wrote the manuscript with input from all authors. All authors edited and approved the final manuscript.

ACKNOWLEDGEMENTS

Special thanks to Nicole Azagury and Mercè Llugany for their assistance in laboratory tasks and thanks to Joana Terés for her help in the collection of *A.thaliana* seeds.

FUNDING INFORMATION

This research was funded by Spanish Ministry of Science and Innovation Project PID2019-10400RB-I00.

DATA AVAILABILITY STATEMENT

The data that support the findings of this study are available from the corresponding author upon reasonable request.

ORCID

Silvia Busoms https://orcid.org/0000-0002-9917-7118

REFERENCES

Al-Mansouri, H. M., & Alhendawi, R. A. M. (2014) Effect of increasing concentration of bicarbonate on plant growth and nutrient uptake by maize plants. *American-Eurasian Journal of Agricultural & Environmental Sciences*, 14 (1), 2014.

Bakker, E.G., Stahl, E.A., Toomajian, C., Nordborg, M., Kreitman, M. & Bergelson, J. (2006) Distribution of genetic variation within and among local populations of *Arabidopsis thaliana* over its species range. *Molecular Ecology*, 15(5), 1405–1418.

Beck, J.B., Schmuts, H. & Schaal, B.A. (2008) Native range genetic variation in *Arabidopsis thaliana* is strongly geographically structures and reflects Pleistocene glacial dynamics. *Molecular Ecology* 17(3), 902–915.

Bergelson, J., Stahl, E., Dudek, S. & Kreitman, M. (1998) Genetic variation within and among populations of *Arabidopsis thaliana*. *Genetics*, 148, 1311–1323.

Bricks, G.C., Osmont, K.S., Shindo, C., Sibout, R. & Hardtke, C.S. (2006) Unequal genetic redundancies in Arabidopsis – a neglected phenomenon? *Trends in Plant Science*, 11(10), 492–498.

Busoms, S., Teres, J., Huang, X. Y., Bomblies, K., Danku, J., Douglas, A., … & Salt, D. E. (2015) Salinity is an agent of divergent selection driving local adaptation of Arabidopsis to coastal habitats. *Plant Physiology*, 168 (3), 915–929.

Busoms, S., Pérez-Martín, L., Terés, J., Huang, X. Y., Yant, L., Tolrà, R., … & Poschenrieder, C. (2023) Combined genomics to discover genes associated with tolerance to soil carbonate. *Plant, cell & environment*, 46 (12), 3986–3998.

DiMario, R.J., Quebedeaux, J.C., Longstreth, D.J., Dassanayake, M., Hartman, M.M. & Moroney, J.V. (2016) The cytoplasmic carbonic anhydrase βCA2 and βCA4 are required for optimal plant growth at low CO2. *Plant Physiology*, 171, 280–293.

DiMario, R.J., Clayton, H., Mukherjee, A., Ludwig, M. & Moroney J.V. (2017) Plant carbonic anhydrases: Structures, locations, evolution, and physiological roles. *Molecular Plant*, 10(1), 30–46.

DiMario, R.J., Machingura, M.C., Waldrop, G.L. & Moroney, J.V. (2018) The many types of carbonic anhydrases in photosynthetic organisms. *Plant Science*, 268, 11–17.

Di Pietro, M., Vialaret, J., Li, G. W., Hem, S., Prado, K., Rossignol, M., … & Santoni, V. (2013). Coordinated post-translational responses of aquaporins to abiotic and nutritional stimuli in Arabidopsis roots. *Molecular & Cellular Proteomics*, 12(12), 3886–3897.

Duan, X., Yu, Y., Duanmu, H., Chen, C., Sun, X., Cao, L., ...& Zhu, Y. (2018) GsSLAH3, a Glycine soja slow type anion channel homolog, positively modulates plant bicarbonate stress tolerance. *Physiologia Plantarum*, 164(2), 145–162.

Fabre, N., Reiter, I. M., Becuwe-linka, N., Genty, B., & Rumeau, D. (2007) Characterization and expression analysis of genes encoding α and β carbonic anhydrases in Arabidopsis. *Plant, cell & environment*, 30(5), 617–629.

Felle H. (1981) A study of the current-voltage relationships of electrogenic active and passive membrane elements in *Riccia fluitans*. *Biochimica et Biophysica Acta*, 646(1):151–60.

Hassani, A., Azapagic, A. & Shokri, N (2021) Global predictions of primary soil salinization under changing climate in the 21st century. *Nature Commununications*, 12, 6663.

Hedrich, R. & Geiger, D. (2017) Biology of SLAC1-type anion channels-from nutrient uptake to stomatal closure. *New Phytologist*, 216(1), 46–61.

Hu, H, Rappel, W J., Occhipinti, R., Ries, A., Böhmer, M., You, L., Xiao, C., Engineer, C.B., Boron, W.F. & Schroeder, J.I. (2015) Distinct cellular locations of carbonic anhydrases mediate carbon dioxide control of stomatal movements. *Plant Physiology*, 169, 1168–1178.

Ignatova, L., Rudenko, N., Zhurikova, E., Borisova-Mubarakshina, M. & Ivanov, B. (2019) *Metabolites*, 9, 73. doi:https://doi.org/10.3390/metabo9040073

Israel, D., Lee, S.H., Robson, T.M. & Zwlazek, J.J. (2022) Plasma membrane aquaporins of the PIP1 and PIP2 subfamilies facilitate hydrogen peroxide diffusion into plant roots. *BMC Plant Biology*, 22, 566.

Jin, C.W., Chen, W.W., Meng, Z.B. & Zheng S.J. (2008) Iron deficiency-induced increase of root branching contributes to the enhanced root ferruc chelate reductase activity. *Journal of Integrative Plant Biology*, 50(12), 1557–1562.

Kupriyanova, E.V., Pronina, N.A. & Los D.A. (2023) Adapting from low to high: An update to CO_2-concentrating mechanisms of cyanobacteria and microalgae. *Plants*, 12, 1569.

Lehmann, J., Jorgensen, M.E., Fratz, S., Müller, H.M., Kusch, J., Scherzer, S., ...& Maierhofer, T. (2021) Acidosis-induced activation of anion channel SLAH3 in the flooding-related stress response of Arabidopsis. *Current Biology*, 31(16) 3575–3585.

Liu, B., Feng, C., Fang, X., Ma, Z., Xiao, C., Zhang, S.,.....& He, K. (2023) The anion channel SLAH3 interacts with potassium channelsto regulate nitroge-potassium homeostasis and the membrane potential in Arabidopsis. *The Plant Cell* 35, 1259–1280.

Livak, K.J. & Schmittgen, T.D. (2001) Analysis of relative gene expression data using real-time quantitative PCR and the $2^{-\Delta\Delta CT}$ method. *Methods*, 25(4), 402–408.

Martín-Barranco, A., Spielmann, J., Dubeaux, G., Vert, G. & Zelazny E. (2020) Dynamic control of the high affinity iron uptake complex in root epidermis cells. *Plant Physiology*, 184, 1236–1250.

Momayyezi, M., McKown, D., Bell, S.C.S. & Guy, R.D. (2020) Emeging roles for carbonic anhydrase in mesophyll conductance and photosynhesis. *The Plant Journal*, 101, 831–844.

Müller, W.E.G., Qiang, L., Schröder, H.C., Hönig, N., Yuan, D., Grebenjuk, V.A., Mussino, F., Giovine, M. & Wang X. (2014) Carbonic anhydrase: a key regulatory and detoxifying enzyme for Karst plants. *Planta*, 239, 213–229.

Qiu, J., Henderson, S. W., Tester, M., Roy, S. J., & Gilliham, M. (2016) SLAH1, a homologue of the slow type anion channel SLAC1, modulates shoot Cl− accumulation and salt tolerance in *Arabidopsis thaliana*. *Journal of Experimental Botany*, 67, 4495–4505.

Parisi, G., Perales, M., Fornasari, M., Colaneri, A., Schain, N., Casati, D., … & Zabaleta, E. (2004) Gamma carbonic anhydrases in plant mitochondria. *Plant Molecular Biology*, 55, 193–207.

Pérez-Martín L., Busoms S., Tolrà R., Poschenrieder C. (2021) Transcriptomics reveals fast changes in salicylate and jasmonate signaling pathways in shoots of carbonate tolerant *Arabidopsis thaliana* under bicarbonate exposure. *International Journal of Molecular Sciences*, 22(3), 1226.

Poschenrieder, C., Fernández, J.A., Rubio, L., Pérez, L., Terés, J. & Barceló, J. (2018) Transport and use of bicarbonate in plants: current knowledge and challenges ahead. *International Journal of Molecular Science*, 19, 1352.

Raven, J.A., Giordano, M., Beardall, J. & Maberly, S.C. (2011) Algal and aquatic plant carbon concentrating mechanisms in relation to environmental change. *Photosynthesis Research*, 109(1–3), 281–96.

Riaz, N. & Guerinot M.L. (2021) All together now: regulation of the iron deficiency response. *Journal of Experimental Botany*, 72(6), 2045–2055.

Rubio, L., García, D., García-Sánchez, M. J., Niell, F. X., Felle, H.H. & Fernández, J. A. (2017) Direct uptake of HCO_3^- in the marine angiosperm *Posidonia oceanica* (L.) Delile driven by a plasma membrane H^+ economy. *Plant Cell Environment*, 40, 2820–2830.

Schmid, K.J., Törjék, O., Meyer, R., Schmuts, H., Hoffmann, M.H. & Altmann, T. (2006) Evidence for a large-scale population structure of *Arabidopsis thaliana* from genome-wide single nucleotide polymorhism markers. *Theoretic and Applied Genetics*, 112, 1104–1114.

Shitov, A. V., Zharmukhamedov, S. K., Shutova, T. V., Allakhverdiev, S. I., Samuelsson, G., & Klimov, V. V. (2011) A carbonic anhydrase inhibitor induces bicarbonate-reversible suppression of electron transfer in pea photosystem 2 membrane fragments. *Journal of Photochemistry and Photobiology B: Biology*, 104(1–2), 366–371.

Stenøien, H.K., Fenster, C.B., Tonteri, A. & Savolainen, O. (2005) Genetic variability in natural populations of *Arabidopsis thaliana* from northern Europe. *Molecular Ecology*, 14, 137–148.

Tagliavini, M. & Rombolà, A.D. (2001) Iron deficiency and chlorosis in orchard and vineyard ecosystems. *European Journal of Agronomy*, 15, 71–92.

Terés J., Busoms S., Perez-Martin L., Luis-Villarroya A., Flis P., Álvarez-Fernández A., Tolrà R., Salt D. & Poschenrieder, C. (2019) Soil carbonate drives local adaptation in *Arabidopsis thaliana*. *Plant Cell & Environment*, 42, 2384–2398.

Tian, W., Hou, C., Ren, Z., Pan, Y., Jia, J., Zhang, H., Bai, F., Zhang, P., Zhu, H., He, Y., Luo, S., Li, L. & Luan S. (2015) A molecular pathway for CO_2 response in Arabidopsis guard cells. *Nature Communications*, 6, 6057.

Vélez-Bermúdez, I.C. & Schmidt, W. (2023) Plant strategies to mine iron from alkaline substrates. *Plant and Soil*, 483, 1–25.

Wahba, M.M., Labib, F. & Zaghloul, A. (2019) Management of calcareous soils in arid regions. *International Journal of Pollution & Environmental Modelling*, 2(5), 248–258.

Wang, M., Zhang, Q., Liu, F.C., Xie, W.F., Wang, G.D., Wang, J., Gao, Q.H. & Duan, K. (2014) Family-wide expression characterization of Arabidopsis beta-carbonic anhydrase genes using qRT-PCR and promoter: *Gus* fusions. *Biochimie*, 97, 219–227.

Wang, N., Dong, X., Chen, Y., Ma, B., Yao, C., Ma, F. & Liu, z. (2020) Direct and bicarbonate-induced iron deficiency differently affect iron translocation in kiwifruit roots. *Plants*, 9(11), 1578.

Weerasooriya, H.N., Longstreth, D.J., DiMario, R.J., Rosati, V., Cassel, B.A. & Moroney, J.V. (2024) Carbonic anhydrases in the cell wall and plasma membrane of *Arabidopsis thaliana* are required for optimal plant growth on low CO_2. *Frontiers in Plant Science*, 11, 1267046.

Wu, H., Zhang, X., Giraldo J.P. & Shabala, S. (2018) It is not all about sodium: revealing tissue specificity and signalling roles of potassium in plant responses to salt stress. *Plant and Soil*, 431, 1–17.

Wu, Y.Y. & Xing, D.K. (2012) Effect of bicarbonate treatment on photosynthetic assimilation of inorganic carbon in two plant species of Moraceae. *Photosynthetica*, 50(4), 587–594.

Wu, Y. & Wu, Y. (2022) The diversification of adaptive strategies for Karst-adaptable plants and the utilization of plant resources in Karst ecosystems. *Agronomy*, 13(8), 2135.

Xu, F., & Yu, F. (2023). Sensing and regulation of plant extracellular pH. *Trends in Plant Science*, 28, 1422–1437.

Zhang, J., Wang, J., Jiang, W., Liu, J., Yang, S., Gai, J., & Li, Y. (2016) Identification and analysis of NaHCO3 stress responsive genes in wild soybean (*Glycine soja*) roots by RNA-seq. *Frontiers in Plant Science*, 7: 1842.

Zhang, H., Yu, F., Xie, P., Sun, S., Qiao, X., Tang, S., Chen, C., Yang, S., Mei, C., Yang, D., Wu, Y., Xia, R., Li, X., Lu, J., Liu, Y., Xie, X., Ma, D., Xu, X., Liang, Z., … Xie, Q. (2023). A Gγ protein regulates alkaline sensitivity in crops. *Science*, 379, 1204.

Zhou, L., Xiang, X., Ji, D., Chen, Q., Ma, T., Wang, J. & Liu, C. (2024) A carbonic anhydrase, ZmCA4, contributes to photosynthetic efficiency and modulates CO_2 signalling gene expression by interacting with aquaporin ZmPIP2,6 in maize. *Plant and Cell Physiology* 65(2), 243–258.

SUPPORTING INFORMATION

Additional supporting information can be found online in the Supporting Information section at the end of this article.

How to cite this article: Pérez-Martín, L., Almira, M.-J., Estrela-Muriel, L., Tolrà, R., Rubio, L., Poschenrieder, C. et al. (2024) A role for root carbonic anhydrase βCA4 in the bicarbonate tolerance of *Arabidopsis thaliana*. *Physiologia Plantarum*, 176(6), e70026. Available from: https://doi.org/10.1111/ppl.70026